Journal of Magnetism and Magnetic Materials 517 (2021) 167344

Contents lists available at ScienceDirect

Journal of Magnetism and Magnetic Materials

journal homepage: www.elsevier.com/locate/jmmm

Research articles

Effect of phase purity on enhancing the magnetic properties of Mn-Bi alloy

Yang Yang[a,b], Jihoon Park[a], Jung Tae Lim[a], Jong-Woo Kim[a,*], Oi Lun Li[b,*], Chul-Jin Choi[a]

[a] Powder & Ceramics Division, Korea Institute of Materials Science, Changwon 51508, Republic of Korea
[b] School of Materials Science and Engineering, Pusan National University, Busan 46241, Republic of Korea

ARTICLE INFO

Keywords:
Rare-earth-free magnet
MnBi LTP
Phase purity
Magnetic properties

ABSTRACT

High purity MnBi magnetic low temperature phase (LTP) were prepared via induction melting, annealing and low energy ball milling. The effects of synthetic parameters and chemical compositions on phase purity and magnetic properties were systematically investigated. A homogenization heat treatment process was employed to increase the fraction of LTP MnBi, which showed notably high saturation magnetization (M_s) of up to 74.8 Am^2/kg with the purity of 97 wt% LTP MnBi. The purity of MnBi is strongly related to the amount of Mn and residual Bi in the annealed ingot. By controlling the residue, the highest phase fraction was obtained with the atomic ratio of $Mn_{56}Bi_{44}$. The maximum energy product $(BH)_{max}$ was recorded 11.7 MGOe under an applied magnetic field of 1.5 T at room temperature, making MnBi a promising rare-earth-free permanent magnet.

1. Introduction

Rare-earth-free MnBi has attracted spotlights nowadays with its high crystal anisotropic field and outstanding magnetic properties, even in the high-temperature range. The low temperature phase (LTP) MnBi crystallizes in the NiAs type hexagonal crystal structure in which the *c*-axis is the easy direction of magnetization and exhibits high magneto-crystalline anisotropy ($K = 1.6 \times 10^6$ $J{\cdot}m^{-3}$) [1–3]. Although the NdFeB magnets have a high maximum energy product $(BH)_{max}$ at room temperature, the low Curie temperature (T_c) is only 583 K and the negative temperature coefficient limits its application ranges at high temperatures [4]. By the way, the MnBi magnet has a higher T_c of 711 K [5] and the unusual positive temperature coefficient of the coercive field [6] makes it a promising candidate for high-temperature applications.

However, synthesizing high purity LTP MnBi has been a critical technical issue for achieving high-performance magnets. The reason why this is challenging is that the difference in melting temperature between Mn and Bi is quite large, about 1000 K and the peritectic reaction occurs in a wide range of temperatures and compositions [7]. Further, Mn is easily to segregate from the Mn-Bi liquid phase through the peritectic reaction at 720 K during the solidification process and the LTP MnBi is decomposed by the eutectic reaction at 535 K [7–9].

In order to overcome these fabrication obstacles and improve the purity of LTP MnBi, many efforts have been made by understanding the microstructure [9,10], particle size control [11,12] and transformation kinetics during the heat treatments [13,14]. In previous reports, X. Zhen *et al.* obtained about 90 wt% of LTP MnBi by induction melting with post annealing at 563 K for 30 h [15]. V.V. Nguyen *et al.* prepared 97 wt% of LTP MnBi by the arc-melting process followed by sintering in vacuum at 573 K [16]. S. Kim *et al.* obtained 98 wt% of LTP MnBi by melt-spun and annealing for 20 h followed the magnetic separation process [17].

Various manufacturing techniques have also been employed to achieve high quality MnBi powders [18–20]. Xie *et al.* prepared sub-micron sized MnBi powders with LTP content up to 96 wt% using low energy ball milling at a cryogenic temperature [18]. A recent result by B. A. Jensen *et al.* shows that the MnBi powders could achieve the $(BH)_{max}$ of 13.0 MGOe using a rather high magnetic field of 9 T at 300 K after melt-spun and low energy ball milling for 8 h [20]. Further, controlling the chemical composition between Mn and Bi is crucial to reduce the unreacted Mn and Bi residue, and thereby enhancing the magnetic property of MnBi. However, with these efforts, the experimental results have not yet reached its theoretical value (17.7 MGOe) [5], so it is necessary to keep developing adequate synthetic processes with optimizing fabrication factors for high performance MnBi magnet.

In this work, the phase purity and magnetic properties of MnBi powders prepared by induction melting have been investigated. Compared with the conventional rapid-solidification process, this process has noticeable advantages in mass production or industrial applications with its simplicity of preparation and higher fabrication yield, etc. At the same time, it is easier to avoid the loss of Mn / Bi at higher synthesis temperature. Fabricated MnBi alloys were then explored in detail about the effects of heat treatments, ball milling processes, and

* Corresponding authors.
E-mail addresses: jwk@kims.re.kr (J.-W. Kim), helenali@pusan.ac.kr (O.L. Li).

https://doi.org/10.1016/j.jmmm.2020.167344
Received 28 February 2020; Received in revised form 22 July 2020; Accepted 22 August 2020
Available online 05 September 2020

further chemical compositions on phase purity critical in obtaining better magnetic properties.

2. Experimental

MnBi powders with nominal compositions $Mn_{55}Bi_{45}$ + x *wt.*% Mn (x = 0 – 7) were prepared using induction melting, post annealing, low energy ball milling, and magnetic separation processes. MnBi ingots were fabricated with high purity Mn and Bi elements (> 99.9%) by induction melting. The obtained ingots were then annealed at 573 K for 24–84 h in an argon atmosphere to obtain high purity LTP MnBi. The annealed ingots were manually crushed using mortar and pestle. The powders were sieved using # 625 mesh screens to obtain initial particles with a size of less than ~ 25 μm. The low energy ball milling has a unique advantage, as the LTP MnBi is easily decomposed during high energy milling. The obtained powders were then milled using low energy ball milling at a rotation speed of 175 rpm from 1 to 9 h. The milling was performed using zirconia balls (5 mm in diameter) with the ball-to-powders weight ratio of 10:1 in ethyl alcohol. To maximize the LTP content, the as-milled powders underwent a magnetic separation process by ethanol for several times to increase magnetic phase purity.

The crystal structures of the as-milled powders were characterized by using X-ray diffraction (XRD) with Cu-K_α radiation. The powder morphology and chemical composition of annealed samples were examined by a field emission scanning electron microscope (FE-SEM) equipped with an Oxford Aztec energy dispersive spectroscopy (EDS) detector. The magnetic properties were measured via vibrating-sample magnetometer (VSM) with maximum applied magnetic field of 1.5 T with a small amount of paraffin wax for powders immobilization.

3. Results and discussion

The XRD patterns of as-casted and 573 K-annealed $Mn_{55}Bi_{45}$ ingots are shown in Fig. 1(a). In contrast to as-casted ingots, the unreacted Mn and Bi appear as minor phases for the annealed ingots, while LTP MnBi presents as the major phase. To investigate the phase identity and weight fraction, the measured XRD patterns were analyzed for all samples using the Rietveld refinement method with the FULLPROF program. As a result, the MnBi in all samples were hexagonal structure with the space group $P6_3/mmc$ and the lattice constants a_0 and c_0 were 4.285 ± 0.002 and 6.115 ± 0.003 Å. The peaks around 27.2° and 43.0° were attributed to the residual Bi and α-Mn phases. For clarity, the phase fractions calculated by Rietveld refinement were listed in Table 1 and plotted in Fig. 1(b). The LTP MnBi phase fraction increased from 88.0 wt% to 92.6 wt% by increasing the annealing time increasing from 24 to 72 h, meanwhile, decreased at longer annealing time. The melting point of Bi (545 K) is lower than the annealing temperature of 573 K, while the melting point of Mn is rather high (1518 K). As a result, it is expected that the segregated Mn reacts with the Bi-rich matrix during annealing, which results in the crystallization of LTP MnBi. Li *et al.* reported a similar phase purity trend increasing with increasing annealing time and reached a maximum value of 89.1 wt% after annealing for 25 h [21]. Because the kinetics of MnBi formation is slow, it is reasonable that a higher fraction of LTP MnBi (92.6 wt%) could be obtained by extending the annealing time to 72 h.

Table 1
The phase fractions of annealed MnBi alloys based on Rietveld refinement.

Annealed time (h)	MnBi (*wt.* %)	Bi (*wt.* %)	α-Mn (*wt.* %)
24	88.0	7.2	4.8
48	90.5	6.0	3.5
72	92.6	4.0	3.4
84	92.2	4.6	3.2

The microstructure of the as-casted and 72 h annealed MnBi alloys were analyzed by FE-SEM in backscattered electron imaging mode, as shown in Fig. 2. Dark grey, black, and light grey regions correspond to the LTP MnBi, Mn and Bi, respectively. For the as-casted alloy, it can be found that most of the unreacted Mn and residual Bi co-exist with a small amount of LTP MnBi. In contrast, for the annealed ingot, the LTP MnBi forms a homogeneous matrix with only a small amount of Bi and Mn residue. Judging by the increased phase of LTP MnBi, it is well agreed with the high purity LTP MnBi confirmed by XRD shown in Fig. 1.

Since the annealed $Mn_{55}Bi_{45}$ ingot still contains a small amount of unreacted Bi, a precise amount of excess Mn is systematically added to effectively promote the reaction with residual Bi and further improve the phase purity. Fig. 3(a) shows the X-ray diffraction patterns of the as-annealed $Mn_{50}Bi_{50}$ and $Mn_{55}Bi_{45}$ ingots, in which the $Mn_{55}Bi_{45}$ ingot contains an excess of 1–7 wt% Mn. For comparison, a large amount of Bi still exists in the $Mn_{50}Bi_{50}$ annealed ingot; however, the $Mn_{55}Bi_{45}$ annealed ingot is mainly comprise LTP MnBi. As the excessive Mn contents increases, Bi peak becomes vivid, indicating reduced LTP portion. The fraction of LTP MnBi is calculated by Rietveld refinements shown in Fig. 3(b). The LTP MnBi phase fraction increases from 92.6 wt % to 97.0 wt% as the excess Mn increases from 0 wt% to 1 wt% and shows a linear decrease as more excess Mn is added. The highest fraction of LTP MnBi in this work was achieved with the excessive 1 wt% Mn(≈$Mn_{56}Bi_{44}$), which is compatible with previously reported composition (~56 *at.*% Mn) fabricated by rapid solidification process or arc

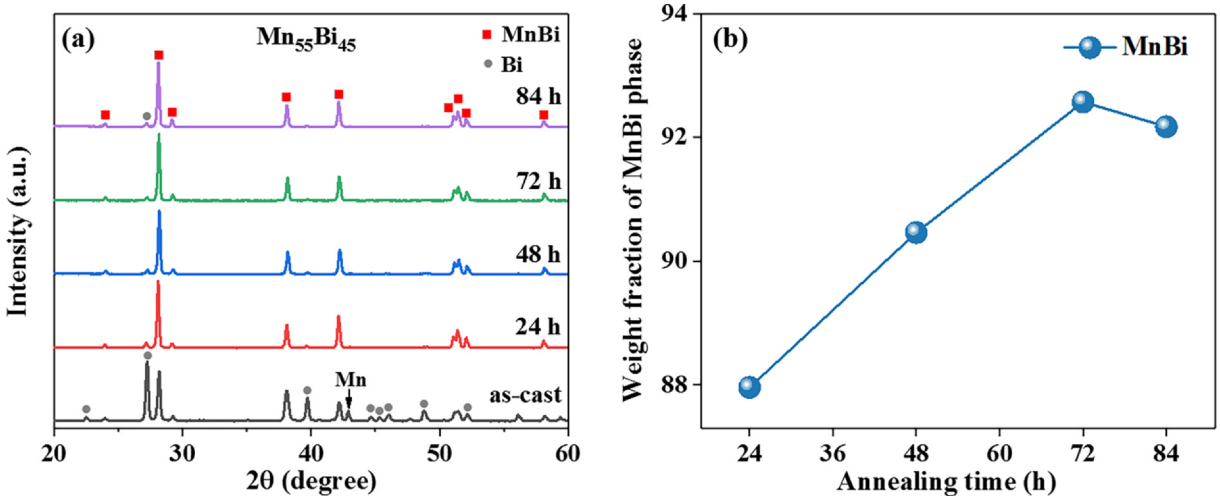

Fig. 1. (a) The XRD patterns and (b) the LTP MnBi weight fraction of the as-casted and different durations annealed $Mn_{55}Bi_{45}$ ingots.

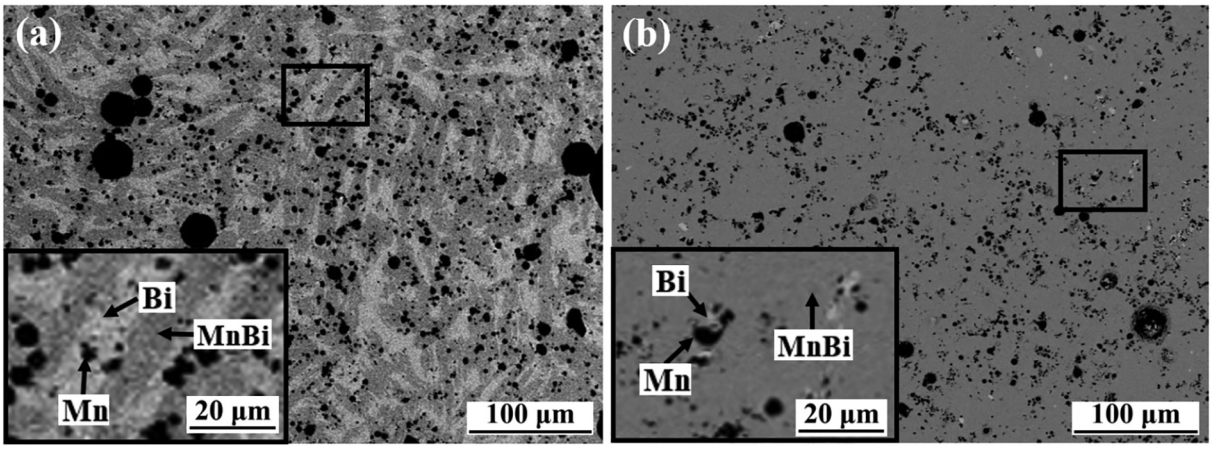

Fig. 2. The SEM observation of the $Mn_{55}Bi_{45}$ ingots: (a) as-casted and (b) annealed for 72 h at 573 K.

melting and heat treatment processes [22,23].

Further optimization process has been done with the chemical composition of $Mn_{56}Bi_{44}$. The low energy ball milling process was employed to enhance its coercivity (H_c) by controlling the particle size. The effect of milling time on particle size and morphology is shown in Fig. 4. The initial powders were crushed and sieved with a size of less than 25 μm. With the milling time increases from 0 to 4 h, the average particle size was decreased gradually. It was found that the particle size of MnBi powders was more homogeneous after 3 h ball milling.

The XRD patterns of the magnetically separated $Mn_{56}Bi_{44}$ powders with various low energy ball milling times, and the fraction variation of LTP MnBi are shown in Fig. 5. As the ball milling time increased, the portion of LTP MnBi is getting decreased from 97 wt% to 75 wt% with the milling time from 1 to 9 h. In the meantime, the residual Bi peak intensity becomes higher, indicating that it is related to the phase decomposition of LTP MnBi due to introduced mechanical energy or stress.

In order to investigate the effect of milling time on magnetic properties, the room temperature demagnetization curves of the magnetic-field aligned $Mn_{56}Bi_{44}$ powders were measured as shown in Fig. 6(a). The theoretical density (8.9 g/cm^3) was used to calculate the maximum energy product $(BH)_{max}$. The H_c, $(BH)_{max}$, and saturation magnetization (M_s) values extracted from the hysteresis loops are plotted as a milling time function as shown in Fig. 6(b). The H_c of the initially crushed powders (< 25 μm) were measured around 0.4 T − 0.5 T. However, the H_c was increased remarkably from 0.83 T to 1.53 T with milling time increased from 1 to 9 h, mainly owing to the refinement of MnBi particle size. In contrast to the coercive field, the M_s was decreased from 74.8 Am^2/kg of the initially crushed powders to 56 Am^2/kg of the 9 h ball milling powders. In general, H_c and M_s are in a trade-off relationship, even though a higher H_c is obtained after ball milling for 9 h, the decrease of M_s value can result in a decreased magnetic property overall. This phenomenon is related to the decomposition of the ferromagnetic LTP MnBi into the nonmagnetic Bi phase, leading to the reduction of the M_s of MnBi powders, likewise discussed in Fig. 5 and previous report [19].

Even though both XRD and magnetic results confirmed the decomposition of the MnBi phase during ball milling, the optimized ball milling conditions in this work were milling for 3 h. With that, MnBi exhibited a high ratio of M_r/M_s reached to 0.97, indicating the possibility of high *c*-axis orientation and proper alignment in bonded MnBi magnet. Further, excellent magnetic properties with M_s of 65.4 Am^2/kg and $(BH)_{max}$ of 11.7 MGOe could be obtained. It is noteworthy that the $(BH)_{max}$ of this work is close to 70% of the theoretical value, which shows that the properties can be enhanced by optimizing the composition and post processes. Therefore, it can be emphasized that the MnBi powders with the minimal magnetic phase decomposition and a smooth demagnetization curve with high H_c have been achieved.

4. Conclusions

MnBi alloy with enhanced magnetic properties was fabricated by

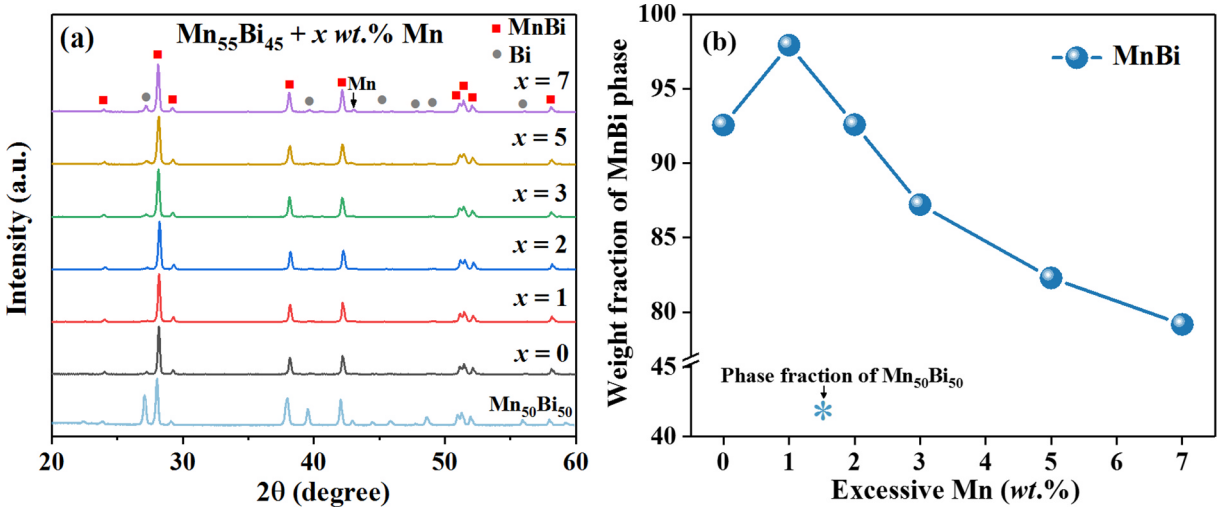

Fig. 3. (a) The XRD patterns and (b) the LTP MnBi fraction of $Mn_{50}Bi_{50}$ and $Mn_{55}Bi_{45}$ + *x* wt.% Mn (*x* = 0, 1, 2, 3, 5 and 7) ingots after annealed for 72 h.

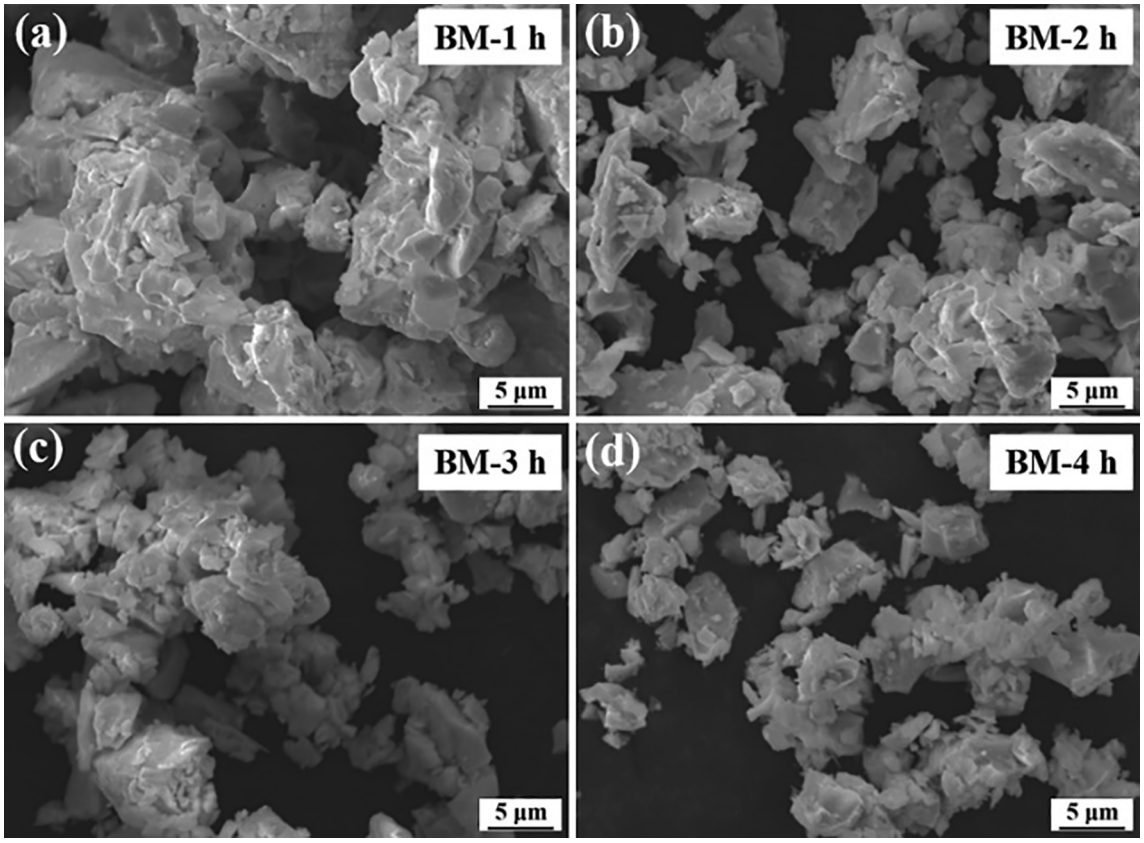

Fig. 4. The SEM images of MnBi powders morphology after ball milling for (a) 1 h, (b) 2 h, (c) 3 h and (d) 4 h, respectively.

induction melting, followed by annealing and low energy ball milling processes. The improved magnetic properties are mainly due to the increased purity of the low temperature phase (LTP) MnBi and the optimized microstructure of the powders. The results showed that the purity of LTP MnBi was as high as 97 wt% and the saturation magnetization (M_s) of $Mn_{56}Bi_{44}$ powders reaches 74.8 Am^2/kg with annealing time of 72 h. The highest coercivity (H_c) of 1.53 T could be obtained by controlling the ball milling time to 9 h with compensation of LTP MnBi fraction due to mechanical stress during ball milling. With the optimized fabrication process, the $Mn_{56}Bi_{44}$ powders showed the maximum energy product $(BH)_{max}$ of 11.7 MGOe with M_s of 65.4 Am^2/kg under an applied magnetic field of 1.5 T at room temperature. The MnBi powders with higher performance and higher purity are crucial for the preparation of MnBi bulk. The ways how to improve purity and phase control of MnBi powders and remarkably enhanced magnetic properties discussed in this work can hopefully open good chances for industrial applications in rare-earth permanent magnet markets or as a gap magnet combined with rare-earth magnets.

Declaration of Competing Interest

The authors declare that they have no known competing financial interests or personal relationships that could have appeared to influence the work reported in this paper.

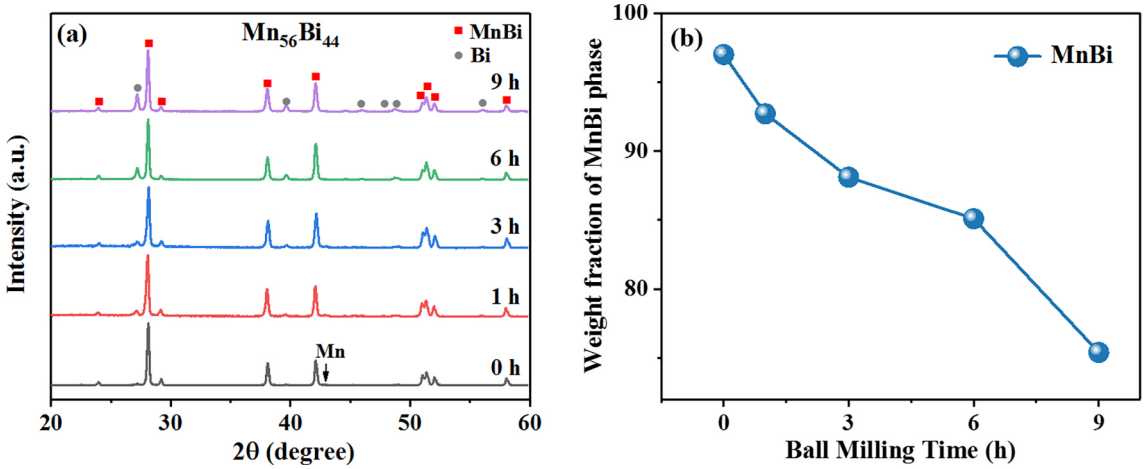

Fig. 5. (a) The XRD patterns and (b) the LTP MnBi fraction of the $Mn_{56}Bi_{44}$ powders ball milling for 1 h, 3 h, 6 h and 9 h, respectively.

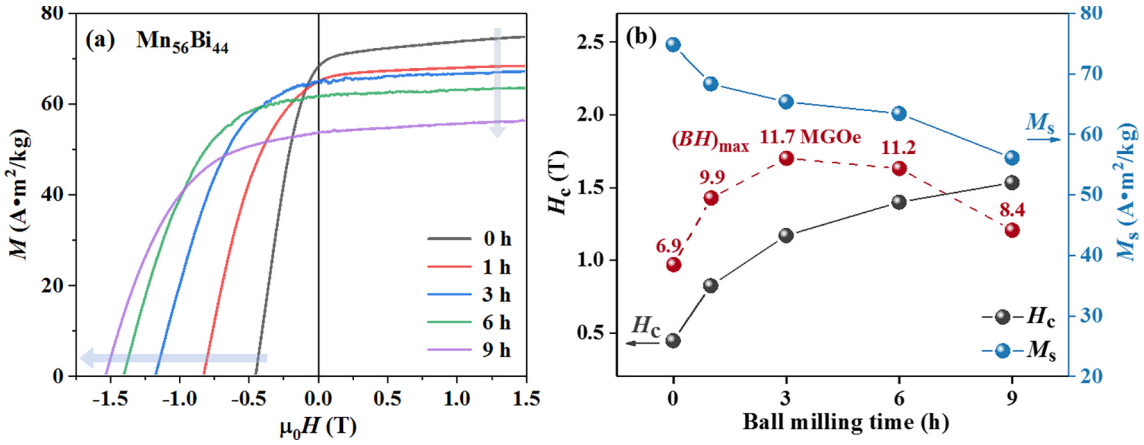

Fig. 6. (a) The demagnetization curves and (b) magnetic properties of the $Mn_{56}Bi_{44}$ ball milling powders for 1 h, 3 h, 6 h and 9 h, respectively.

Acknowledgements

This work was mostly supported by Future Materials Discovery Program through the National Research Foundation of Korea (NRF) funded by the Ministry of Science and ICT (2016M3D1A1027835) and partly by Fundamental Research Program (PNK6940) of the Korea Institute of Materials Science (KIMS).

References

[1] B. Roberts, Neutron diffraction study of the structures and magnetic properties of manganese bismuthide, Phys. Rev. 104 (1956) 607–616.
[2] A. Andresen, W. Hälg, P. Fischer, E. Stoll, The magnetic and crystallographic properties of MnBi studied by neutron diffraction, Acta Chem. Scand. 21 (1967) 1543–1554.
[3] X. Guo, X. Chen, Z. Altounian, J.O. Ström-Olsen, Magnetic properties of MnBi prepared by rapid solidification, Phys. Rev. B. 46 (1992) 14578–14582.
[4] T. Akiya, H. Kato, M. Sagawa, K. Koyama, Enhancement of coercivity in Al and Cu added Nd-Fe-B sintered magnets by high field annealing, Mater. Sci. Eng. 1 (2009) 012034–012039.
[5] J. Park, Y.-K. Hong, J. Lee, W. Lee, S.-G. Kim, C.-J. Choi, Electronic structure and maximum energy product of MnBi, Metal 4 (2014) 455–464.
[6] Y.B. Yang, X.G. Chen, S. Guo, A.R. Yan, Q.Z. Huang, M.M. Wu, D.F. Chen, Y.C. Yang, J.B. Yang, Temperature dependences of structure and coercivity for melt-spun MnBi compound, J. Magn. Magn. Mater. 330 (2013) 106–110.
[7] J. Cui, J.-P. Choi, G. Li, E. Polikarpov, J. Darsell, N. Overman, M. Olszta, D. Schreiber, M. Bowden, T. Droubay, M.J. Kramer, N.A. Zarkevich, L.L. Wang, D.D. Johnson, M. Marinescu, I. Takeuchi, Q.Z. Huang, H. Wu, H. Reeve, N.V. Vuong, J.P. Liu, Thermal stability of MnBi magnetic materials, J. Phys.: Condens. 26 (2014) 064212.
[8] T. Chen, Contribution to the equilibrium phase diagram of the Mn-Bi system near MnBi, J. Appl. Phys. 45 (1974) 2358–2360.
[9] Y.-C. Chen, S. Sawatzki, S. Ener, H. Sepehri-Amin, A. Leineweber, G. Gregori, F. Qu, S. Muralidhar, T. Ohkubo, K. Hono, O. Gutfleisch, H. Kronmüller, G. Schütz, E. Goering, On the synthesis and microstructure analysis of high performance MnBi, AIP Advances 6 (2016) 125301.
[10] Y.-C. Chen, G. Gregori, A. Leineweber, F. Qu, C.-C. Chen, T. Tietze, H. Kronmüller, G. Schütz, E. Goering, Unique high-temperature performance of highly condensed MnBi permanent magnets, Scripta Mater. 107 (2015) 131–135.
[11] J. Cao, Y.L. Huang, Y.H. Hou, Z.Q. Shi, X.T. Yan, Z.C. Zhong, G.P. Wang, Microstructure and magnetic properties of MnBi alloys with high coercivity and significant anisotropy prepared by surfactant assisted ball milling, J. Magn. Magn. Mater. 473 (2019) 505–510.
[12] K. Kanari, C. Sarafidis, M. Gjoka, D. Niarchos, O. Kalogirou, Processing of magnetically anisotropic MnBi particles by surfactant assisted ball milling, J. Magn. Magn. Mater. 426 (2017) 691–697.
[13] N. Poudyal, X.B. Liu, W. Wang, V.V. Nguyen, Y.L. Ma, K. Gandha, K. Elkins, J.P. Liu, K.W. Sun, M.J. Kramer, J. Cui, Processing of MnBi bulk magnets with enhanced energy product, AIP Advances 6 (2016) 056004.
[14] Z. Xiang, T.L. Wang, S.J. Ma, L.W. Qian, Z.Y. Luo, Y.M. Song, H.W. Yang, W. Lu, Microstructural evolution and phase transformation kinetics of MnBi alloys, J. Alloy. Comp. 741 (2018) 951–956.
[15] Z. Xiang, Y.M. Song, D. Pan, Y.L. Shen, L.W. Qian, Z.Y. Luo, Y.S. Liu, H.W. Yang, H. Yan, W. Lu, Coercivity enhancement and magnetization process in $Mn_{55}Bi_{45}$ alloys with refined particle size, J. Alloy. Comp. 744 (2018) 432–437.
[16] V.V. Nguyen, N. Poudyal, X.B. Liu, J.P. Liu, K. Sun, M.J. Kramer, J. Cui, Novel processing of high-performance MnBi magnets, Mater. Res. Express 1 (2014) 036108.
[17] S. Kim, H. Moon, H. Jung, S.-M. Kim, H.-S. Lee, C.-Y. Haein, W. Lee, Magnetic properties of large-scaled MnBi bulk magnets, J. Alloy. Comp. 708 (2017) 1245–1249.
[18] W. Xie, E. Polikarpov, J.-P. Choi, M.E. Bowden, K. Sun, J. Cui, Effect of ball milling and heat treatment process on MnBi powders magnetic properties, J. Alloy. Comp. 680 (2016) 1–5.
[19] N.V. Rama Rao, G.C. Hadjipanayis, Influence of jet milling process parameters on particle size, phase formation and magnetic properties of MnBi alloy, J. Alloy. Comp. 629 (2015) 80–83.
[20] B.A. Jensen, W. Tang, X.B. Liu, A.I. Nolte, G. Ouyang, K.W. Dennis, J. Cui, Optimizing composition in MnBi permanent magnet alloys, Acta Mater. 181 (2019) 595–602.
[21] B.B. Li, Y.L. Ma, B. Shao, C.H. Li, D.M. Chen, J.C. Sun, Q. Zheng, X.G. Yin, Preparation and magnetic properties of anisotropic MnBi powders, J. Phys. B. 530 (2018) 322–326.
[22] J. Cui, J.-P. Choi, E. Polikarpov, M.E. Bowden, W. Xie, G.S. Li, Z.M. Nie, N. Zarkevich, M.J. Kramer, D. Johnson, Effect of composition and heat treatment on MnBi magnetic materials, Acta Mater. 79 (2014) 374–381.
[23] J. Cui, J.-P. Choi, G. Li, E. Polikarpov, J. Darsell, M.J. Kramer, N.A. Zarkrvich, L.L. Wang, D.D. Johnson, M. Marinescu, Q.Z. Huang, H. Wu, N.V. Vuong, J.P. Liu, Development of MnBi permanent magnet: neutron diffraction of MnBi powder, J. Appl. Phys. 115 (2014) 17A743.